

RESEARCH COMMUNICATION

Regulation of Ca^{2+} -release-activated Ca^{2+} current (I_{crac}) by ryanodine receptors in inositol 1,4,5-trisphosphate-receptor-deficient DT40 cellsKirill KISELYOV^{*1}, Dong Min SHIN^{*}, Nikolay SHCHEYNIKOV^{*}, Tomohiro KUROSAKI[†] and Shmuel MUALLEM^{*}^{*}Department of Physiology, University of Texas Southwestern Medical Center, 5323 Harry Hines Boulevard, Dallas, TX 75390-9040, U.S.A., and [†]Department of Molecular Genetics, Institute for Liver Research, Kansai Medical University, Moriguchi 570-8506, Japan

Persistence of capacitative Ca^{2+} influx in inositol 1,4,5-trisphosphate (IP_3) receptor (IP_3R)-deficient DT40 cells ($\text{DT40}^{\text{IP}_3\text{R}^{-/-}}$) raises the question of whether gating of Ca^{2+} -release activated Ca^{2+} current (I_{crac}) by conformational coupling to Ca^{2+} -release channels is a general mechanism of gating of these channels. In the present work we examined the properties and mechanism of activation of I_{crac} Ca^{2+} current in wild-type and $\text{DT40}^{\text{IP}_3\text{R}^{-/-}}$ cells. In both cell types passive depletion of internal Ca^{2+} stores by infusion of EGTA activated a Ca^{2+} current with similar characteristics and time course. The current was highly Ca^{2+} -selective and showed strong inward rectification, all typical of I_{crac} . The activator of ryanodine receptor (RyR),

cADP-ribose (cADPR), facilitated activation of I_{crac} , and the inhibitors of the RyRs, 8-*N*-cADPR, ryanodine and Ruthenium Red, all inhibited I_{crac} activation in $\text{DT40}^{\text{IP}_3\text{R}^{-/-}}$ cells, even after complete depletion of intracellular Ca^{2+} stores by ionomycin. Wild-type and $\text{DT40}^{\text{IP}_3\text{R}^{-/-}}$ cells express RyR isoforms 1 and 3. RyR levels were adapted in $\text{DT40}^{\text{IP}_3\text{R}^{-/-}}$ cells to a lower RyR3/RyR1 ratio than in wild-type cells. These results suggest that IP_3Rs and RyRs can efficiently gate I_{crac} in DT40 cells and explain the persistence of I_{crac} gating by internal stores in the absence of IP_3Rs .

Key words: calcium influx, patch-clamp, ryanodine receptor.

INTRODUCTION

The mechanism of activation of store-operated Ca^{2+} channels (SOCs) in response to depletion of intracellular Ca^{2+} stores is a topic of intense investigation. The main proposed routes of communication between Ca^{2+} stores and the plasma membrane (PM) Ca^{2+} channels are by a soluble messenger [1], Ca^{2+} -release channels as sensing and transduction elements [conformational coupling (C-C)] [2] and fusion of Ca^{2+} -influx-channel-containing vesicles with the PM [3]. The SOCs represent a heterogeneous subset of PM Ca^{2+} channels. The best-characterized form of SOC is the Ca^{2+} -release-activated Ca^{2+} current, I_{crac} [4,5], which is also present in cells of immune system [6,7].

I_{crac} channels have unique biophysical characteristics, the most prominent of which are very high selectivity for Ca^{2+} over univalent cations, low conductance in the presence of bivalent cations and inward rectification of the Ca^{2+} current (reviewed in [5]). Since the molecular identity of the SOCs is not known, model systems were used to study their gating mechanism. Recently we demonstrated that the human homologues of the *Drosophila* Trp channel TRPC3 stably expressed in HEK cells are coupled to, and are gated by, inositol 1,4,5-trisphosphate receptors (IP_3Rs) [8,9]. These findings were confirmed [10,11] and extended to native SOCs [12,13], supporting gating of SOC by C-C to Ca^{2+} -release channels.

Recent findings raised the possibility that gating by C-C is not a general gating mechanism of SOCs. Thus activation of Ca^{2+} influx by store depletion persisted in the chicken B lymphocyte cell line DT40 from which all isoforms of IP_3R were deleted

($\text{DT40}^{\text{IP}_3\text{R}^{-/-}}$) [14–16] and from which stores IP_3 was unable to release Ca^{2+} [14]. However, it is important to note that other Ca^{2+} -release channels, such as the ryanodine-receptor (RyR)- or the nicotinic acid-adenine dinucleotide phosphate (NAADP)-activated channels [17], may also couple to SOCs and gate their activity. Indeed, in previous work we showed that RyRs can couple to hTRPC3 and regulate their activity and the activity of I_{crac} [18]. Importantly, coupling of hTRPC3 channels to IP_3Rs and RyRs is mutually exclusive [18]. However, because the cells used in our previous studies expressed both RyRs and IP_3Rs , it is not clear whether RyRs gated the SOCs directly or by facilitating Ca^{2+} store depletion while IP_3Rs present in the same sub-pool activated the SOCs. In this respect, the $\text{DT40}^{\text{IP}_3\text{R}^{-/-}}$ cells provide an excellent system to study gating of the SOCs by RyRs.

Here we report that passive depletion of intracellular Ca^{2+} stores activated I_{crac} in both wild-type and $\text{DT40}^{\text{IP}_3\text{R}^{-/-}}$ cells. The two cell lines express two RyR isoforms, namely RyR1 and RyR3. In both cell types, activation of I_{crac} is facilitated by activation of RyR, and inhibition of the RyRs inhibited I_{crac} activation. These findings demonstrate that RyRs can gate I_{crac} independently of the IP_3Rs and provide further support for gating of Ca^{2+} influx channels by Ca^{2+} -release channels.

EXPERIMENTAL

Solutions

The standard bath solution for intracellular Ca^{2+} concentration ($[\text{Ca}^{2+}]_i$) measurement contained (in mM): 140 NaCl, 5 KCl,

Abbreviations used: I_{crac} , Ca^{2+} -release-activated Ca^{2+} current; IP_3R , inositol 1,4,5-trisphosphate (receptor); $\text{DT40}^{\text{IP}_3\text{R}^{-/-}}$, IP_3R -deficient DT40 cells; cADPR, cADP-ribose; SOC, store-operated Ca^{2+} channel; PM, plasma membrane; C-C, conformational coupling; NAADP, nicotinic acid-adenine dinucleotide phosphate; $[\text{Ca}^{2+}]_i$, intracellular Ca^{2+} concentration; RT-PCR, reverse transcriptase PCR; Rya, ryanodine; RuR, Ruthenium Red.

¹ To whom correspondence should be sent (e-mail kirill.kiselyov@UTSouthwestern.edu).

1 MgCl₂, 10 Hepes/KOH (adjusted to pH 7.4 with NaOH), 10 glucose and either 1 mM CaCl₂ or 0.1 mM EGTA (Ca²⁺-free). The extracellular solution for whole-cell current measurement contained (in mM): 140 sodium aspartate, 5 NaCl, 10 Hepes/KOH (adjusted to pH 7.4 with NaOH), 1 mM MgCl₂ and 1 or 10 mM CaCl₂. The pipette solution contained (in mM): 140 caesium aspartate, 5 NaCl, 1 MgCl₂, 1 ATP, 10 Hepes, 0.1, 0.5, 2 or 10 EGTA/CsOH (adjusted to pH 7.3 with CsOH). cADPR, ryanodine (Rya) and Ruthenium Red (RuR) were from Calbiochem, IP₃ was from Alexis, and 8-*N*-cADPR was from Molecular Probes.

Cells

Wild-type and DT40^{IP₃R^{-/-}} cells were kept in culture essentially as described previously [14]. In brief, cells were grown in RPMI-1640 medium supplemented with 10% (v/v) fetal-calf serum, 1% chicken serum, 1% penicillin/streptomycin and 400 μg/ml G-418. The medium was changed three times each week. All cell-culture reagents, except G-418 (Life Sciences), were from Atlanta Biologicals, Norcross, GA, U.S.A.

Measurement of [Ca²⁺]_i

Cells in suspension were loaded with 2 μM fura 2 acetoxymethyl ester by 30 min incubation at 37 °C. After loading, cells were washed and incubated in extracellular medium for 40 min to allow completion of fura 2 acetoxymethyl ester hydrolysis. Immediately before the experiment, cells were immobilized by attachment on to polylysine-coated coverslips. Cells were illuminated by an alternating 340/380 nm light delivered every 0.5 s. Fluorescence intensity at 510 nm was measured with a DeltaRAM fluorimetric system (PTI Inc., Monmouth Junction, NJ, U.S.A.). Changes in [Ca²⁺]_i are presented as the change in the ratio of fluorescence intensity at 340 and 380 nm.

Electrophysiology

Current was recorded using an Axopatch 200A patch-clamp amplifier (Axon Instruments, Foster City, CA, U.S.A.) and digitized at 2 kHz. Throughout the experiment the membrane potential was held at 0 mV to minimize Ca²⁺-dependent inactivation of Ca²⁺ current. The membrane conductance was probed with consecutive rapid (250 ms) alteration of membrane potentials ('RAMPs') from -120 to +60 mV delivered every 2 s. Pipettes had resistance between 5 and 7 MΩ when they were filled with an intracellular solution, and seal resistance was always more the 8 GΩ. Current recording and analysis was performed with the use of pClamp 6.0.3 (Axon Instruments) software suite. To calculate τ20%I_{max} (the time elapsed from the start of the recording until the current reaches 20% of its maximal value), current recordings were fitted with the equation:

$$I = I_2 + (I_1 - I_2) / \{1 + \exp[(t - t_0)/dt]\}$$

where *I*₁ and *I*₂ are current amplitudes at the beginning of recording and at the maximal stable amplitude and *t* is the time. Fitting was performed using the MicroCal Origin 5.0 software (Microcal Software, Northampton, MA, U.S.A.). Experiments were carried out at room temperature (22–24 °C). Results are given as means ± S.E.M.

Reverse transcriptase PCR (RT-PCR)

To analyse expression of RyRs, mRNA and then cDNA were prepared from wild-type and DT40^{IP₃R^{-/-}} cells using Trizol RNA

extraction and RT-PCR Superscript kits respectively. The primers used to amplify RyR1 were:

Sense: 5' TCGTGGCCTTCAACTTCTTC

Antisense: 3' TCTCCATGTCTCCTTACC (size 309 bp)

and the primers used to amplify RyR3 were:

Sense: 5' CATCAAGGCAGTGGGTTCTT

Antisense: 3' CGGAAGTCAATGGGCATACT (size 497 bp)

Actin was amplified with the following primers:

Sense: 5' TTTGAGACCTTCAACACCCC

Antisense: 3' TCTCCTGCTCGAAATCCAGT (size 310)

Samples were incubated at 95 °C for 2 min then cycled 35 times for RyRs and 20 times for actin at 95 °C for 1 min, 60 °C for 1 min and 72 °C for 1 min. Reactions were terminated by incubation at 72 °C for 5 min and cooling. In preliminary experiments we determined the linear range for the amount of mRNA and the cycle numbers to be used. Then the amount of cDNA was titrated on the basis of the signal obtained with actin. Samples for analysis of the RT-PCR products for RyRs and actin mRNA were taken at the linear phase of the PCR reaction. Multiple cDNA preparations were used to eliminate any possibility that the difference in RyR levels is due to any step up to the RT-PCR reaction. This allowed quantification of the differences between wild-type and DT40^{IP₃R^{-/-}} cells.

Immunoprecipitation and Western blot

Lysates were prepared from wild-type and DT40^{IP₃R^{-/-}} cells as described previously [18]. Since RyRs could not be reproducibly detected by Western blot of lysates from DT40 cells, the receptors were first immunoprecipitated by incubating 250 μl of lysate with 250 μl of supernatant from the 34C hybridoma developed by J. Airey and J. Sutko (Department of Pharmacology, University of Nevada School of Medicine, Reno, NV, U.S.A.) and purchased from the Hybridoma Bank, University of Iowa, Iowa City, IA, U.S.A. After 30 min, 25 μl of Sepharose A beads were added and the samples were incubated overnight at 4 °C. The beads were washed three times and RyRs were released by heating the beads at 70 °C for 10 min in 15 μl of sample buffer. After SDS/PAGE RyRs were detected by blotting with the same antibodies. Microsomes prepared from rat skeletal muscle were used as positive controls.

RESULTS AND DISCUSSION

In the first stage of the present studies we sought to characterize the Ca²⁺ influx and the current induced by store depletion in wild-type and DT40^{IP₃R^{-/-}} cells. In agreement with previous reports [14–16] wild-type, but not DT30^{IP₃R^{-/-}}, cells responded to stimulation of phospholipase C with the M4 antibodies, confirming the lack of functional IP₃-mediated Ca²⁺ release in DT40^{IP₃R^{-/-}} cells (results not shown). Figures 1(A) and 1(B) show that store depletion initiated by application of 1 μM ionomycin to cells incubated in Ca²⁺-free medium induces similar Ca²⁺ influx in both wild-type and DT40^{IP₃R^{-/-}} cells. Similar results have been reported previously [14–16]. To test a possible role of RyRs in activation or maintenance of store-operated Ca²⁺ influx, we tested the effect of the RyR inhibitors Rya [22] and RuR [23] on the influx. Figure 1(C) shows that pretreatment of DT40^{IP₃R^{-/-}} cells with 20 μM Rya inhibited store-dependent Ca²⁺ influx by as much as 45% (*n* = 5). Inhibition of RyRs by RuR does not require pretreatment and RuR can be applied after full activation of the influx. Figure 1(D) shows that RuR (30 or

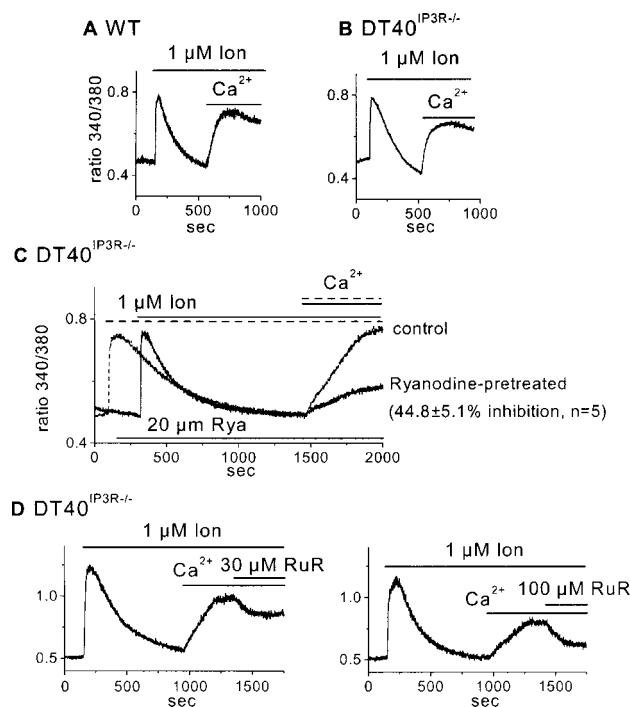


Figure 1 Role of RyRs in store-operated Ca^{2+} influx in wild-type and $\text{DT40}^{\text{IP}_3\text{R}^{-/-}}$ cells

(A) and (B) show the effect of store depletion by ionomycin on Ca^{2+} influx into wild-type and $\text{DT40}^{\text{IP}_3\text{R}^{-/-}}$ cells, respectively. (C) Demonstrates that inhibition of RyR by pretreatment of $\text{DT40}^{\text{IP}_3\text{R}^{-/-}}$ cells with $20 \mu\text{M}$ Rya inhibits store-operated Ca^{2+} influx. (D) Depicts the inhibition of store-dependent Ca^{2+} influx by RuR in $\text{DT40}^{\text{IP}_3\text{R}^{-/-}}$ cells.

$100 \mu\text{M}$) inhibits ionomycin-induced Ca^{2+} entry in $\text{DT40}^{\text{IP}_3\text{R}^{-/-}}$ cells. RuR also inhibited Ca^{2+} influx in wild-type cells (results not shown). Interestingly, RuR was somewhat more effective in inhibiting Ca^{2+} influx into $\text{DT40}^{\text{IP}_3\text{R}^{-/-}}$ than wild-type DT40 cells. In $\text{DT40}^{\text{IP}_3\text{R}^{-/-}}$ cells, $30 \mu\text{M}$ RuR inhibited Ca^{2+} influx by $48.1 \pm 5.5\%$ ($n = 5$), whereas in wild-type cells the inhibition averaged $33.9 \pm 3.1\%$ ($n = 4$). It is possible that the differences in the effects of RuR may reflect differences in the contribution of RyRs to regulation of Ca^{2+} influx in the two cell types.

The finding that inhibition of RyRs inhibits store-operated Ca^{2+} entry in $\text{DT40}^{\text{IP}_3\text{R}^{-/-}}$ cells raises the possibility that RyRs are expressed and regulate the activity of SOCs in these cells. In a previous study we showed that RyR-mediated Ca^{2+} release activates I_{crac} [18]. Therefore we analysed the expression of RyRs in wild-type and $\text{DT40}^{\text{IP}_3\text{R}^{-/-}}$ cells. First, the types of RyRs expressed in DT40 cells were identified by RT-PCR. Figure 2 shows that both cell lines express mRNA coding for the RyR1 and RyR3 isoforms. Interestingly, when calculated relative to actin mRNA, the levels of RyR mRNA for RyR1 were similar in the two cell types (Figure 2A), but the level of mRNA for RyR3 (Figure 2B) was lower by about $59 \pm 7\%$ in $\text{DT40}^{\text{IP}_3\text{R}^{-/-}}$ relative to wild-type cells (summarized in Figure 1D; $n = 5$ for wild-type and $n = 6$ for $\text{DT40}^{\text{IP}_3\text{R}^{-/-}}$ cells).

The level of RyR protein could not be accurately analysed at the present time owing to a lack of antibodies that recognize specific RyR isoforms in DT40 cells. However, to demonstrate expression of RyRs, the proteins were immunoprecipitated by an antibody that recognizes all RyR isoforms, and RyRs in the immunoprecipitate were analysed by Western blot. Figure 1(E) shows expression of RyR protein in wild-type and $\text{DT40}^{\text{IP}_3\text{R}^{-/-}}$

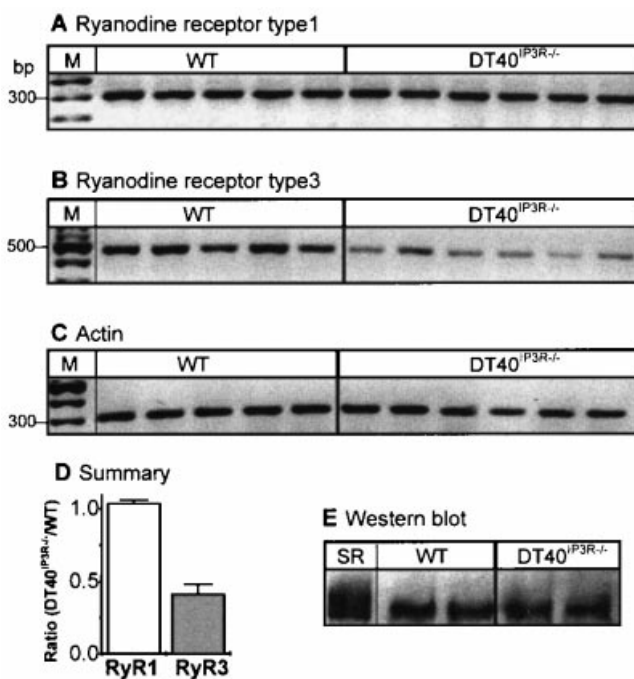


Figure 2 RT-PCR and Western-blot analysis of RyRs in DT40 cells

The primers listed in the Experimental section were used to amplify RyR1 (A), RyR3 (B) and actin (C) in five cDNA preparations from wild-type and six cDNA preparations from $\text{DT40}^{\text{IP}_3\text{R}^{-/-}}$ cells. (D) Summarizes the results of the experiments in (A) and (B) as the ratio of each RyR isoform in the two cell types corrected for actin expression. Intensities were determined by densitometry. (E) RyRs were immunoprecipitated and analysed by Western blot as detailed in the Experimental section (results are representative of three independent experiments).

cells. If the lower level of mRNA for RyR3 in $\text{DT40}^{\text{IP}_3\text{R}^{-/-}}$ cells is reflected in lower RyR3 protein, it is possible that expression of RyRs in $\text{DT40}^{\text{IP}_3\text{R}^{-/-}}$ cells was adjusted in response to deletion of IP_3Rs . The increase in the RyR1/RyR3 ratio in $\text{DT40}^{\text{IP}_3\text{R}^{-/-}}$ cells may suggest that RyR1 is more important for communication with I_{crac} than RyR3.

To characterize and compare the Ca^{2+} current induced by store depletion in wild-type and $\text{DT40}^{\text{IP}_3\text{R}^{-/-}}$ cells, we performed several experiments using the whole-cell mode of the patch-clamp technique. In these experiments, passive store depletion was achieved by infusing the cells with an increasing concentration of the Ca^{2+} chelator EGTA. The extracellular solution contained 10 mM Ca^{2+} and 140 mM Na^+ as the permeable cations. Figures 3(A) and 3(B) show representative recording of the Ca^{2+} currents activated by EGTA in the two cell types. Infusion of 10 mM EGTA resulted in rapid development of the current. Maximal current activation was attained within $100\text{--}150 \text{ s}$ of break-in (Figures 1A and 1B, bottom panels). Lower concentrations of EGTA activated Ca^{2+} currents with a slower onset and smaller amplitude. In both cell types, a concentration of EGTA as low as 0.5 mM was able to partially activate the Ca^{2+} current (Figures 1A and 1B, middle traces). The potency of EGTA to deplete the stores in the DT40 cell lines is higher than that reported in other cell types, including T cells [6,7]. Nevertheless, similar to the findings with the $[\text{Ca}^{2+}]_i$ measurement, there was no difference in the onset time of the current between wild-type and $\text{DT40}^{\text{IP}_3\text{R}^{-/-}}$ cells. The amplitude of the current was slightly higher in $\text{DT40}^{\text{IP}_3\text{R}^{-/-}}$ cells, probably due to their larger size as compared with wild-type cells.

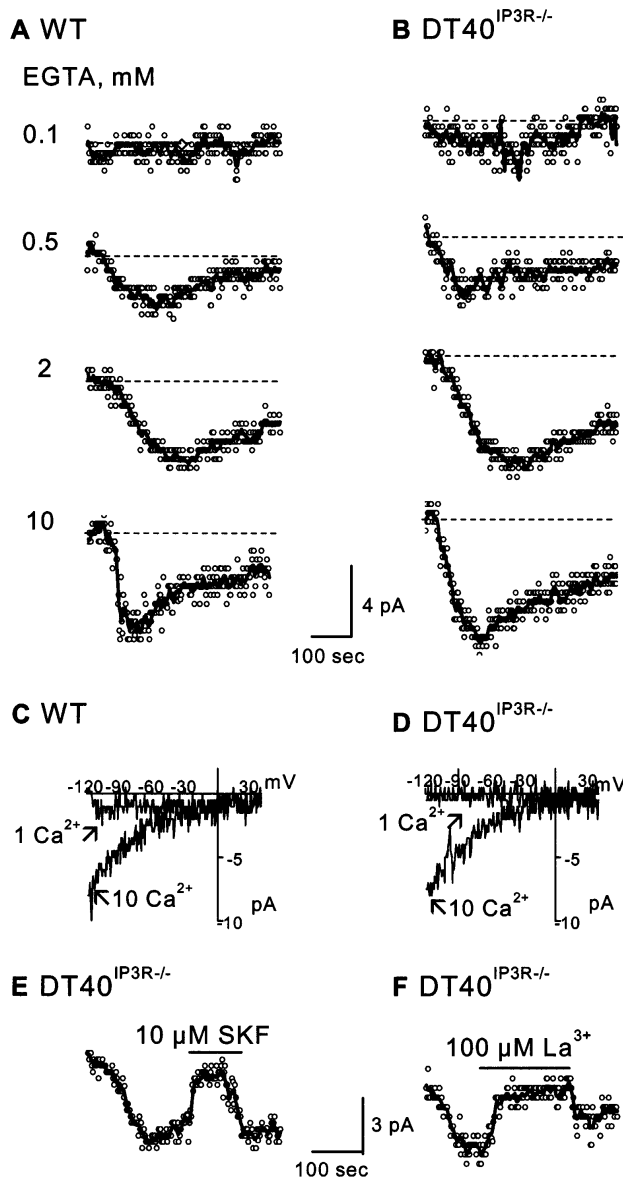


Figure 3 Activation of I_{crac} in wild-type and $\text{DT40}^{\text{IP}_3\text{R}^{-/-}}$ cells

(A) Wild-type (WT) and (B) $\text{DT40}^{\text{IP}_3\text{R}^{-/-}}$ show the current activated by store depletion with increasing concentrations of EGTA. Current values recorded at -100 mV are presented. The thick-line traces were obtained by averaging five consecutive points from corresponding current traces. (C) Wild-type (WT) and (D) $\text{DT40}^{\text{IP}_3\text{R}^{-/-}}$ show that the current is an inward-rectifying Ca^{2+} current. Similar behaviour was observed in more than 40 experiments with each cell type. SKF 96365 (E, $n = 6$) and La^{3+} (F, $n = 5$) inhibited the current in $\text{DT40}^{\text{IP}_3\text{R}^{-/-}}$ cells.

The properties of the currents recorded in wild-type and $\text{DT40}^{\text{IP}_3\text{R}^{-/-}}$ cells are compared in Figures 3(C) and 3(D). The current was highly selective for Ca^{2+} and showed strong inward rectification, similar to the well-characterized properties of I_{erac} [4,6,7]. Therefore the Ca^{2+} release-activated Ca^{2+} current in DT40 cells will henceforth be referred to as I_{erac} . No I_{erac} current was observed when the concentration of Ca^{2+} in the extracellular solution was decreased to 1 mM (Figures 3C and D). The I_{erac} current in wild-type (results not shown) and $\text{DT40}^{\text{IP}_3\text{R}^{-/-}}$ cells was inhibited by $10 \mu\text{M}$ SKF 96365 (Figure 3E) and $100 \mu\text{M}$ La^{3+} (Figure 3F). Both agents are commonly used as inhibitors of I_{erac} [19].

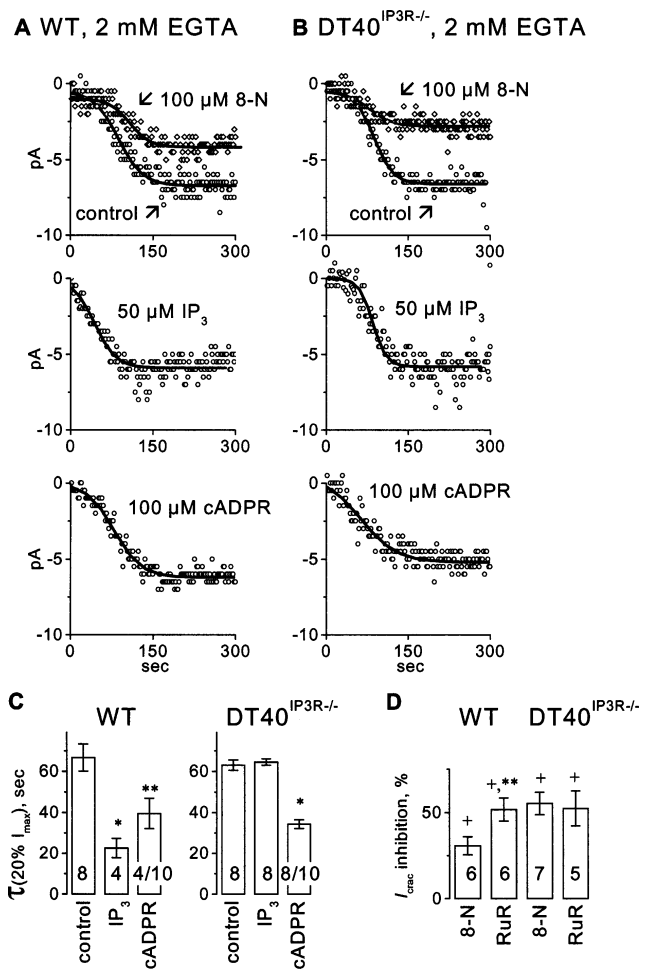


Figure 4 Role of RyRs in I_{erac} activation in wild-type and $\text{DT40}^{\text{IP}_3\text{R}^{-/-}}$ cells

(A) Wild-type (WT) and (B) $\text{DT40}^{\text{IP}_3\text{R}^{-/-}}$ show individual examples, and (C) and (D) summarize the results of multiple experiments. In each panel (representative of five to ten separate experiments) the upper traces are the controls and current recorded with 8-*N*-cADPR (8-N) in the pipette, the middle traces show the effect of IP_3 and the lower traces the effect of cADPR on the time course of I_{erac} activation. The thick lines represent fits of the corresponding records as described in the Experimental section. The times needed for activation of 20% of the current under each condition are summarized in (C) and (D). The averaged effects of 8-*N*-cADPR on current amplitude are shown in (D). In (C), * indicates $P < 0.01$ and ** indicates $P < 0.05$ relative to the respective control. In (D), + indicates $P < 0.05$ relative to control and ** indicates $P < 0.05$ relative to wild-type DT40 cells.

Expression of RyRs in DT40 cells led us to determine whether I_{erac} is regulated by RyRs in these cells. For these experiments we characterized the delay before current onset, which was observed in all experiments performed under the conditions of I_{erac} recording (eight to ten experiments under each condition). The time elapsed from the start of the recording until the current reaches 20% of its maximal value ($\tau_{20\% I_{\text{max}}}$) was calculated by fitting the current traces to the equation given in the Experimental section and was used to compare the kinetics of activation of I_{erac} under different experimental conditions.

To assess the involvement of RyRs in I_{erac} activation, the cells were infused with RyR activators and inhibitors and their effect on the time profile of I_{erac} activation was determined. The top panels in Figures 4(A) and 4(B) illustrate typical I_{erac} current activation induced by infusion of 2 mM EGTA into wild-type and $\text{DT40}^{\text{IP}_3\text{R}^{-/-}}$ cells. The $\tau_{20\% I_{\text{max}}}$ averaged 66.7 ± 6.6 s

($n = 8$) in wild-type and 63.0 ± 2.5 s ($n = 8$) in DT40^{IP₃R^{-/-}} cells. Including IP₃ in the pipette solution was used to activate IP₃R. Co-infusion of 50 μM IP₃ with 2 mM EGTA reduced the initial delay in the development of I_{crac} to 22.6 ± 4.8 s ($n = 4$, $P < 0.05$) in wild-type cells (Figure 4C). As expected, IP₃ had no effect on the time profile of I_{crac} activation in DT40^{IP₃R^{-/-}} cells, with an averaged $\tau_{20\% I_{\max}}$ of 64.6 ± 1.5 s ($n = 8$), which is no different from that measured in the absence of IP₃.

In contrast with IP₃, the RyR activator cADPR was effective in both cell types. Figures 4(A) and 4(B) demonstrate typical recording of I_{crac} induced by 100 μM cADPR in wild-type and DT40^{IP₃R^{-/-}} cells. cADPR had no effect on the amplitude of the current, but it significantly reduced the delay before onset of I_{crac}. On average, cADPR decreased the $\tau_{20\% I_{\max}}$ to 39.5 ± 7.4 s ($n = 4$, $P < 0.05$) in wild-type and to 34.4 ± 2.2 s ($n = 8$, $P < 0.05$) in DT40^{IP₃R^{-/-}} cells (Figure 4C). Interestingly, this effect was observed in eight out of ten experiments in DT40^{IP₃R^{-/-}} cells, but in only four out of ten experiments in wild-type cells. The characteristics of the I_{crac} current induced by EGTA alone, by IP₃, and by cADPR were indistinguishable (results not shown).

In the next set of experiments we tested the effect of the RyR inhibitors 8-N-cADPR [20] and RuR [23] on the dynamics of I_{crac} activation by passive store depletion. It is evident from the representative current traces in Figures 4(A) and 4(B) that infusion of 8-N-cADPR at 100 μM significantly delayed the development of I_{crac} current and decreased its amplitude. Similar results were obtained with 30 μM RuR in the pipette. The decreased amplitude of I_{crac} precluded accurate estimation of the lag time of I_{crac} activation in cells treated with the RyR inhibitors. Therefore Figure 4(D) summarizes the effect of 8-N-cADPR and RuR on the amplitude of I_{crac} in the two cell types. RuR reduced I_{crac} amplitude by $51.8 \pm 6.7\%$ and $52.4 \pm 10.1\%$ in wild-type and DT40^{IP₃R^{-/-}} cells respectively. Interestingly, 8-N-cADPR reduced I_{crac} amplitude in DT40^{IP₃R^{-/-}} cells more than in wild-type cells ($55.2 \pm 6.5\%$ inhibition in DT40^{IP₃R^{-/-}} cells and $28.4 \pm 9.1\%$ inhibition in wild-type cells, $P < 0.05$). However, it was noteworthy that neither of the inhibitors used completely blocked I_{crac} in DT40^{IP₃R^{-/-}} cells. This raises the interesting possibility that Ca²⁺-release channels other than IP₃Rs and RyRs, for example, NAADP-activated channels [17], can gate I_{crac}.

In the present studies we used DT40^{IP₃R^{-/-}} cells to show that activation of RyR facilitates the development of I_{crac} and, conversely, inhibition of RyRs suppresses I_{crac} activation induced by passive store depletion. Importantly, the RyR inhibitors were also effective in reducing I_{crac} current when intracellular Ca²⁺ stores were depleted. This suggests an active role of RyRs in regulation of I_{crac}. Furthermore, the profile of RyR expression in DT40^{IP₃R^{-/-}} cells was different from that in the parental cells. These results suggest that RyRs regulate I_{crac} in DT40 cells and may have a more prominent role in DT40^{IP₃R^{-/-}} cells. In previous work, we showed that RyRs can gate the TRPC3 channels and influence store-dependent Ca²⁺ current in HSG cells [18]. However, since the IP₃- and Rya-sensitive pools can overlap [21], we were unable to exclude the possibility that Ca²⁺ release triggered by activation of RyRs activated SOCs coupled to IP₃Rs present in the same sub-pool. The ability to show regulation of SOCs in the IP₃Rs-deficient DT40^{IP₃R^{-/-}} cells provides conclusive evidence that RyRs can regulate the activity of I_{crac}.

Another important implication of the present findings is that the DT40^{IP₃R^{-/-}} cells survived deletion of all IP₃Rs, probably because the cells express RyRs and are able to gate I_{crac} activity and maintain communication between internal stores and the PM by coupling of I_{crac} channels to RyRs. In addition, how passive depletion of Ca²⁺ from internal stores of DT40^{IP₃R^{-/-}} cells

by thapsigargin can activate capacitative Ca²⁺ entry remains a mystery [14–16]. These findings raised the question of whether Ca²⁺-release channels, in particular IP₃Rs, can indeed gate I_{crac} by C-C [15]. The results of the present work solve this puzzle: RyRs can mediate gating of I_{crac} channels by passive store depletion in DT40^{IP₃R^{-/-}} cells.

This work was supported by grant 0130268N from the American Heart Association to K.K. and National Institutes of Health grants DK38938 and DE12309 to S.M. T.K. was supported by grants from the Ministry of Education, Science, Sports and Culture of Japan.

REFERENCES

- Randriamampita, C. and Tsien, R. Y. (1993) Emptying of intracellular Ca²⁺ stores releases a novel small messenger that stimulates Ca²⁺ influx. *Nature (London)* **364**, 809–814
- Irvine, R. F. (1990) 'Quantal' Ca²⁺ release and the control of Ca²⁺ entry by inositol phosphates – a possible mechanism. *FEBS Lett* **263**, 5–9
- Yao, Y., Ferrer-Montiel, A. V., Montal, M. and Tsien, R. Y. (1999) Activation of store-operated Ca²⁺ current in *Xenopus* oocytes requires SNAP-25 but not a diffusible messenger. *Cell (Cambridge, Mass.)* **98**, 475–485
- Hoth, M. and Penner, R. (1992) Depletion of intracellular calcium stores activates a calcium current in mast cells. *Nature (London)* **355**, 353–356
- Parekh, A. B. and Penner, R. (1997) Store depletion and calcium influx. *Physiol. Rev.* **77**, 901–930
- Zweifach, A. and Lewis, R. S. (1993) Mitogen-regulated Ca²⁺ current of T lymphocytes is activated by depletion of intracellular Ca²⁺ stores. *Proc. Natl. Acad. Sci. U.S.A.* **90**, 6295–6299
- Kerschbaum, H. and Cahalan, M. (1999) Single-channel recording of a store-operated Ca²⁺ channel in Jurkat T lymphocytes. *Science* **283**, 836–839
- Kiselyov, K., Xu, X., Mozhayeva, G. N., Kuo, T., Pessah, I., Mignery, G. A., Zhu, X., Birnbaumer, L. and Muallem, S. (1998) Functional interaction between InsP3 receptors and store-operated Htrp3 channels. *Nature (London)* **396**, 478–482
- Kiselyov, K., Mignery, G., Zhu, M. X. and Muallem, S. (1999) The N-terminal domain of the IP₃ receptor gates store-operated hTrp3 channels. *Mol. Cell* **4**, 423–429
- Boulay, G., Brown, D. M., Qin, N., Jiang, M., Dietrich, A., Zhu, M. X., Chen, Z., Birnbaumer, M., Mikoshiba, K. and Birnbaumer, L. (1999) Modulation of Ca²⁺ entry by polypeptides of the inositol 1,4,5-trisphosphate receptor (IP₃R) that bind transient receptor potential (TRP): evidence for roles of TRP and IP₃R in store depletion-activated Ca²⁺ entry. *Proc. Natl. Acad. Sci. U.S.A.* **96**, 14955–14960
- Zhang, Z., Tang, J., Tikunova, S., Johnson, J. D., Chen, Z., Qin, N., Dietrich, A., Stefani, E., Birnbaumer, L. and Zhu, M. X. (2001) Activation of Trp3 by inositol 1,4,5-trisphosphate receptors through displacement of inhibitory calmodulin from a common binding domain. *Proc. Natl. Acad. Sci. U.S.A.* **98**, 3168–3173
- Zubov, A. I., Kaznacheeva, E. V., Nikolaev, A. V., Alexeenko, V. A., Kiselyov, K., Muallem, S. and Mozhayeva, G. N. (1999) Regulation of the miniature plasma membrane Ca²⁺ channel I_{min} by inositol 1,4,5-trisphosphate receptors. *J. Biol. Chem.* **274**, 25983–25985
- Ma, H. T., Patterson, R. L., van Rossum, D. B., Birnbaumer, L., Mikoshiba, K. and Gill, D. L. (2000) Requirement of the inositol trisphosphate receptor for activation of store-operated Ca²⁺ channels. *Science* **287**, 1647–1651
- Sugawara, H., Kurosaki, M., Takata, M. and Kurosaki, T. (1997) Genetic evidence for involvement of type 1, type 2 and type 3 inositol 1,4,5-trisphosphate receptors in signal transduction through the B-cell antigen receptor. *EMBO J.* **16**, 3078–3088
- Broad, L. M., Braun, F. J., Lievreumont, J. P., Bird, G. S., Kurosaki, T. and Putney, Jr, J. W. (2001) Role of the phospholipase C-inositol 1,4,5-trisphosphate pathway in calcium release-activated calcium current and capacitative calcium entry. *J. Biol. Chem.* **276**, 15945–15952
- Ma, H. T., Venkatchalam, K., Li, H. S., Montell, C., Kurosaki, T., Patterson, R. L. and Gill, D. L. (2001) Assessment of the role of the inositol 1,4,5-trisphosphate receptor in the activation of transient receptor potential channels and store-operated Ca²⁺ entry channels. *J. Biol. Chem.* **276**, 18888–18896
- Yusufi, A. N., Cheng, J., Thompson, M. A., Chini, E. N. and Grande, J. P. (2001) Nicotinic acid-adenine dinucleotide phosphate (NAADP) elicits specific microsome Ca²⁺ release from mammalian cells. *Biochem. J.* **353**, 531–536
- Kiselyov, K. I., Shin, D. M., Wang, Y., Pessah, I. N., Allen, P. D. and Muallem, S. (2000) Gating of store-operated channels by conformational coupling to ryanodine receptors. *Mol. Cell.* **6**, 421–431
- Merritt, J. E., Armstrong, W. P., Benham, C. D., Hallam, T. J., Jacob, R., Jaxa-Chamiec, A., Leigh, B. K., McCarthy, S. A., Moores, K. E. and Rink, T. J. (1990) SK&F 96365, a novel inhibitor of receptor-mediated calcium entry. *Biochem. J.* **271**, 515–522

- 20 Rakovic, S., Cui, Y., Iino, S., Galione, A., Ashamu, G. A., Potter, B. V. and Terrar, D. A. (1999) An antagonist of cADP-ribose inhibits arrhythmogenic oscillations of intracellular Ca^{2+} in heart cells. *J. Biol. Chem.* **274**, 17820–17827
- 21 Khodakhah, K. and Armstrong, C. M. (1997) Inositol trisphosphate and ryanodine receptors share a common functional Ca^{2+} pool in cerebellar Purkinje neurons. *Biophys. J.* **73**, 3349–3357
- 22 Feher, J. J. and Lipford, G. B. (1985) Mechanism of action of ryanodine on cardiac sarcoplasmic reticulum. *Biochim. Biophys. Acta* **813**, 77–86
- 23 Pessah, I. N., Waterhouse, A. L. and Casida, J. E. (1985) The calcium–ryanodine receptor complex of skeletal and cardiac muscle. *Biochem. Biophys. Res. Commun.* **128**, 449–456
-

Received 27 June 2001/13 September 2001; accepted 19 September 2001